Supporting information

A novel method to synthesize BiSI uniformly coated with rGO by chemical bonding and its application as a supercapacitor electrode material

Huapeng Sun‡[a,b], Xufeng Xiao‡[b], Veronica Celorrio[c], Zhenfu Guo[d], Yue Hu[b], Caroline Kirk*[a] and Neil Robertson*[a]

[a.] *School of Chemistry and EaStCHEM, University of Edinburgh, King's Buildings, David Brewster Road, Edinburgh, Scotland EH9 3FJ, UK Address here.*

[b.] *Wuhan National Laboratory for Optoelectronics (WNLO), Huazhong University of Science and Technology (HUST), Wuhan 430074, China.*

[c.] *Diamond Light Source Ltd, Harwell Science and Innovation Campus, Oxfordshire, Didcot OX11 0DE, UK*

[d.] *Hebei North university, Zhangjiakou 075000, Hebei, P. R. China.*

Experimental section

Characterization

Powder X-Ray diffraction (PXRD) data were collected using a Bruker (D2 Advance) diffractometer with Cu-Kα radiation (λ = 1.5418 Å), at room temperature over a 2-theta range of 5° to 60°, with a stepsize of 0.1° and a count time of 0.45s per step. X-ray photoelectron spectra were acquired using a Thermo Scientific (VG Sigma Probe) XPS spectrometer with monochromatic Al-Kα as the source of X-rays. Scanning electron microscopy was carried out using a Zeiss (SIGMA HD VP) Field Emission-Scanning Electron microscope (SEM) operating with an accelerating voltage of 10 kV. Transmission Electron Microscopy (TEM) and Electron Dispersive Spectroscopy (EDS) were carried using a FEI Titan Themis microscope operating with an accelerating voltage of 200 kV. Nitrogen adsorption experiments were carried out to determine specific surface areas of the samples using a JWGB SCI. & TECH BK132F automatic adsorption instrument. After analysis based on the Brunauer-Emmett-Teller (BET) equation: [1]

$$\frac{1}{V\left[(P_0/P)-1\right]}=\frac{1}{V_m c}+\frac{1}{V_m c(P/P_0)}$$

where P and P0 are the equilibrium and the saturation pressure of the adsorption at the temperature of adsorption, V is the adsorbed gas quantity, Vm is the maximum monolayer adsorption quantity, c is the BET constant. Raman spectra were acquired using a Renishaw in Via Raman Microscope with an excitation laser wavelength of 785 nm and a spectral resolution of approximately 1 cm^{-1}.

XANES and EXAFS spectra were recorded in transmission mode at the Bi L3-edge (13418 eV), on beamline B18 at the Diamond Light Source operating with a ring energy 3 GeV and at a current of 300 mA. The monochromator comprises a Si (111) crystal operating in Quick EXAFS mode. Calibration of the monochromator was carried out using a Bi foil. All measurements were collected *in situ*, using our custom designed electrochemical cells based on the design of a published reference[2] and connected to an OctoStat200 (Ivium). The data were analyzed using the Athena and Arthemis programs.[3] The spectra was calibrated using the Bi foil response.Measurement of electrochemical properties

The working electrode for the three-electrode system was prepared by mixing BiSI-rGO,BiSI-coated and BiSI powder with activated charcoal powder and PTFE powder in 1 mL ethanol as the solvent to make a final activated material : charcoal: PTFE mixture with a weight ratio of 90:5:5. The resulting suspended solution was sonicated until homogenized, and around 200 μL was drop-coated onto 1 cm^2 conductive carbon paper (ELAT, NuVant Systems Inc.) substrate and dried at 90 ℃ for 6 hours. The

active mass of deposited BiSI-rGO, BiSI-coated, and BiSI electrodes were 2.3 mg, 2.6 mg, and 2.4mg, respectively, used for all subsequent calculations. In the three-electrode system, Ag/AgCl (3.0 M KCl) and a Pt wire were used as the reference and counter electrode, respectively with 3.0 M KOH aqueous electrolyte. Cyclic voltammetry (CV), galvanostatic charge/discharge measurements and electrochemical impedance spectroscopy (EIS) were carried out using an Autolab electrochemical work station with FRA2 module using General Purpose Electrochemical System (GPES) and Frequency Response Analyser (FRA) software.

The specific capacity were calculated from the slope of the discharge curves according to:[4]

$$Specific\ capacity\ (C/g) = \frac{i \times \Delta t}{m}$$

where i is the constant current (A), dV/dt is the slope of the discharge curve taken in the voltage range 0-1 V for consistency, Area is the average geometric area of the two electrodes (cm^2) and m is combined mass of the active material on the working electrode.

Before assembling the hybrid ASC supercapacitor, the two working electrodes with the mass loadings were optimized to be m^+/m^- ratios about 1:2, were soaked into 3 M KOH for 3 h. The energy density (E) and power density (P) were calculated on the basis of the total mass of the active materials of the two electrodes according to the following equations:

$$E = \frac{I \int V dt}{3.6m}$$

$$P = \frac{3600E}{\Delta t}$$

where I is the discharge current, V is the voltage window, t is the time for full discharge and m is the mass of working electrode for the assembled ASC devices.

The Faradaic efficiency be calculated using the formula m = (M×I×t) / (N×F)

Where m is the theoretical yield (current efficiency); M stands for the Molar mass (weight of displaced element in grams); I represents the current in Amperes; t is the time in seconds; N is the Oxidation state (number of displaceable electrons per atom) and F is Faraday's constant; F=96487 Coulombs.

Results and discussion

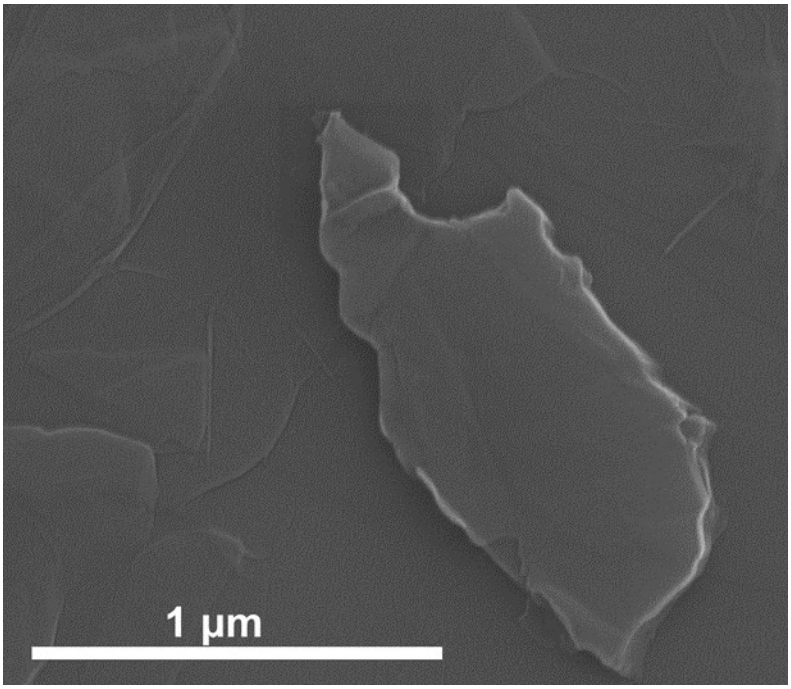

Figure S1. SEM image of GO nanosheet that was used to synthesize BiSI-rGO

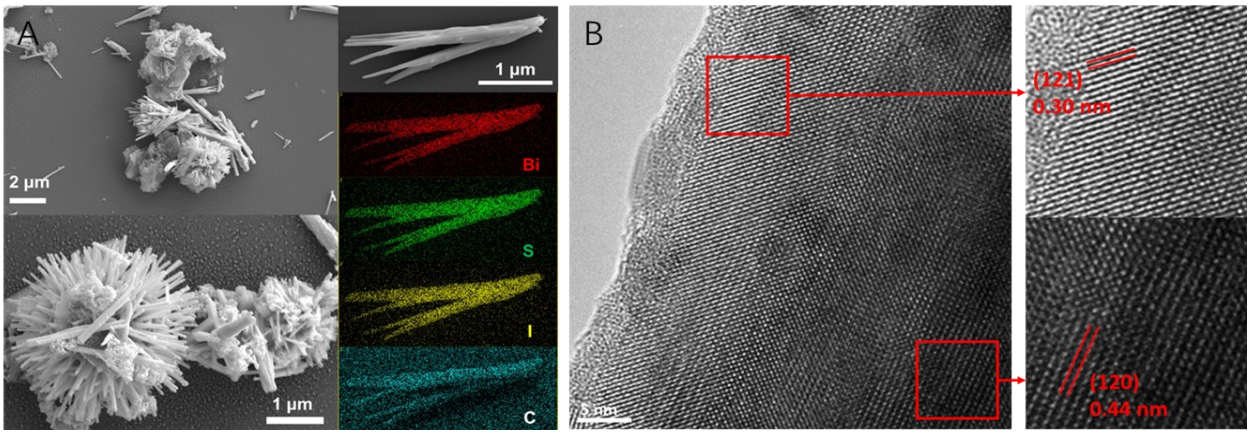

Figure S2. SEM image of BiSI-mix sample with EDS mapping(A), and partial enlarged high-resolution TEM image image of BiSI-rGO sample (B).

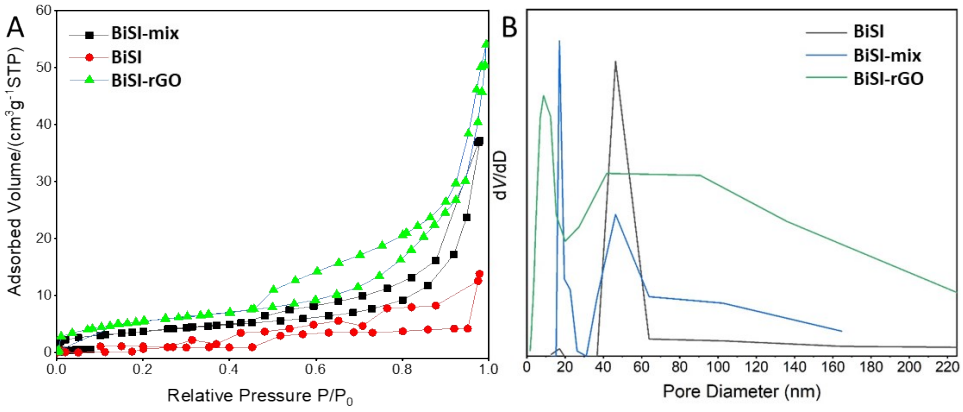

Figure S3. Nitrogen adsorption-desorption isotherms for BiSI, BiSI-coated and BiSI-rGO powder

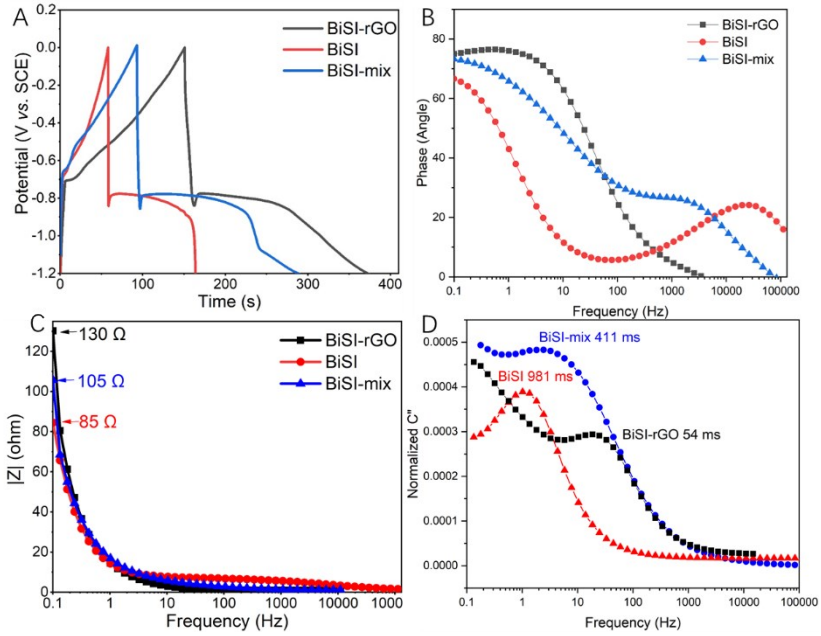

Figure S4. (A) GCD plots of BiSI, BiSI-rGO and BiSI-mix electrodes at 1 A g^{-1}, the bode phase plots (B and C), and the relaxation time constant (D) of the BiSI, BiSI-rGO and BiSI-mix electrodes.

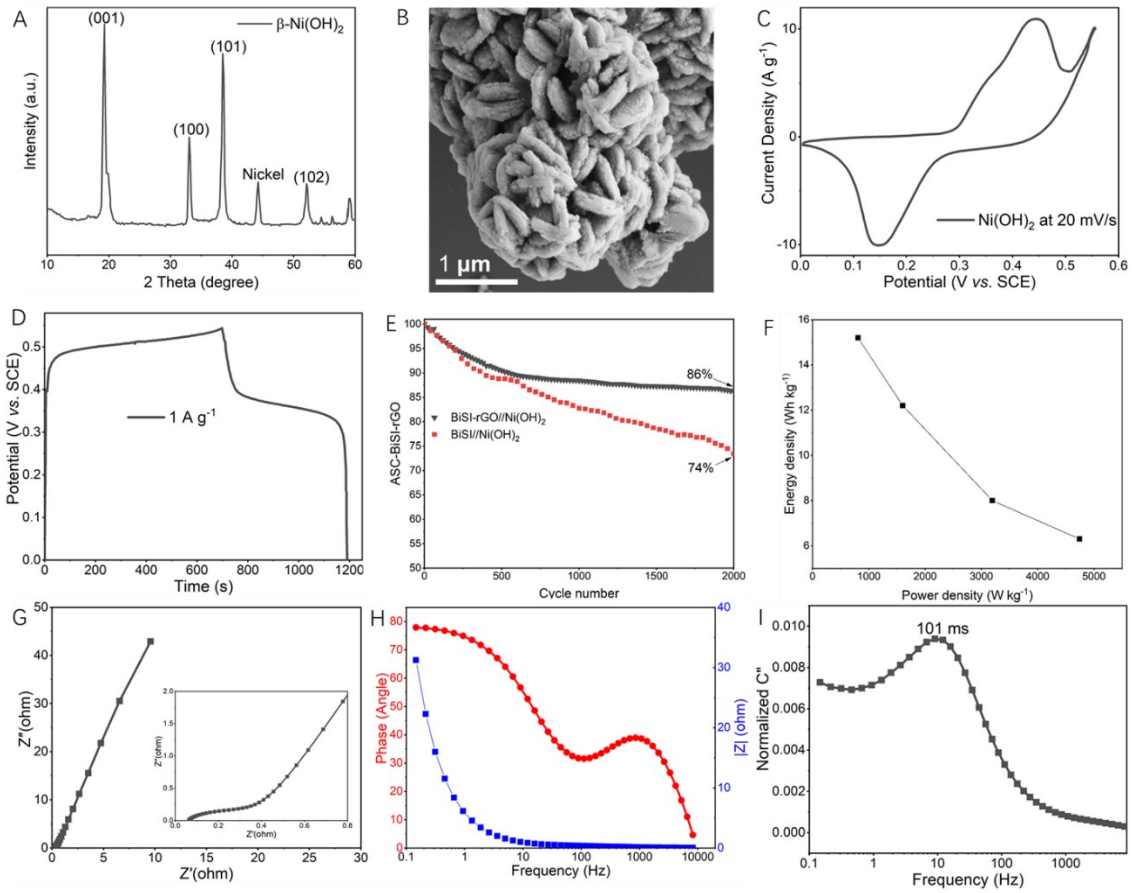

Figure S5, The XRD pattern of positive electrode (A), (B) SEM image of $Ni(OH)_2$, CV scan (C) and GCD plot (D) of positive electrode, (E) Cycle performance of BISI-rGO HSC, (F) BiSI HSC devices and Ragone diagram (F) of BISI-rGO HSC, EIS plot (G), Bode phase plots (H) and relaxation time constant (I) of the HSC devices

Table S1. Linear combination fit analysis results for in situ XANES spectra of the prepared electrodes recorded at the Bi L_{III} edge in absent of electrolyte and any applied potential.

Sample	Bi species composition / %		Mean Oxidation state	R_{factor}
	Bi (0)	Bi (III)		
BiSI-rGO	48.1 ± 1.4	51.9 ± 2.6	1.6 ± 0.1	0.002
BiSI	37.5 ± 5.8	62.5 ± 1.7	1.9 ± 0.1	0.004

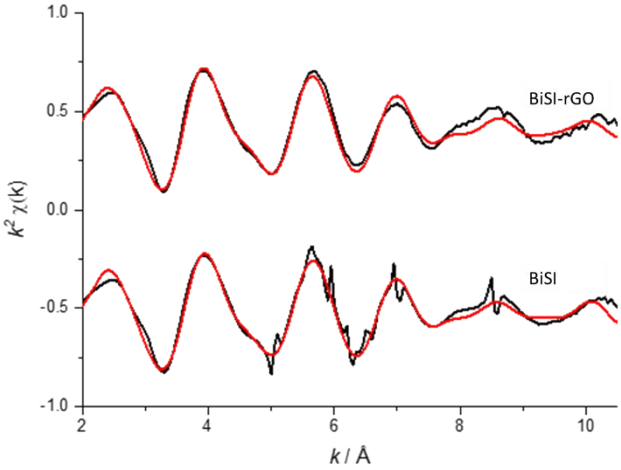

Figure S6. Data (black line) and fits (red line) of the k2-weighted EXAFS signals in k-space for BiSI-rGO and BiSI electrodes.

Table S2. Relative energy shift and the best fit results from the structural analysis of BiSI-rGO and BiSI dry electrodes at the Bi LIII-edge. N is the coordination number, R is the interatomic distance and σ2 is the Debye-Waller factor. Rf is the R-factor, which represents the relative error of the fit and data. Fitting range: 2.8 < k < 10.4; 1.17 < R < 4.20.

	Shell	N	R / Å	σ^2 x 10^3 / Å^2	S_0^2	ΔE_0 / eV	R_f
BiSI-rGO_dry	Bi-S	3	2.66 ± 0.04	16.9.4 ± 4.9	1.02 ± 0.30	-0.3 ± 2.5	0.038
	Bi-I_1	2	3.20 ± 0.12	18.0 ± 7.8			
	Bi-I_2	2	3.74 ± 0.27	22.5 ± 20.2			
	Bi-S	1	3.91 ± 0.35	15.7 ± 8.9			
	Bi-Bi	2	3.97 ± 0.12	13.4 ± 12.7			
BiSI_dry	Bi-S	3	2.66 ± 0.03	16.1 ± 3.4	0.96 ± 0.20	-0.19 ± 1.7	0.019
	Bi-I_1	2	3.19 ± 0.06	15.9 ± 4.3			
	Bi-I_2	2	3.68 ± 0.17	20.9 ± 20.5			
	Bi-S	1	3.86 ± 0.17	12.6 ± 6.4			
	Bi-Bi	2	3.96 ± 0.09	12.7 ± 8.9			

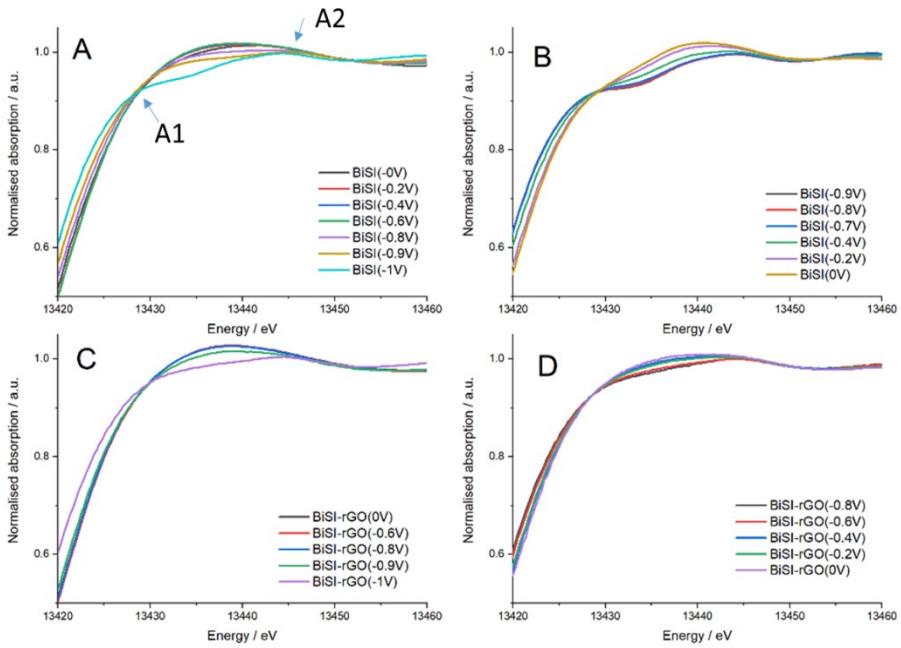

Figure S7. Enlarge view of XANES spectra post edge for BiSI (A, B) and BiSI-rGO (C, D) in 1 M KOH under a cathodic (A, C) and anodic (B, D) scan.

Table S3. Linear combination fit analysis results for in situ XANES spectra of BiSI-rGO recorded at the Bi L_{III} edge 1 M KOH solution at various applied potentials.

BiSI-rGO	Bi species composition / %		Mean Oxidation state	R_{factor}
	Bi (0)	Bi (III)		
KOH	26.9 ± 1.0	73.1 ± 2.4	2.2 ± 0.1	0.001
-600 mV	23.8 ± 0.9	76.2 ± 2.4	2.3 ± 0.1	0.001
-800 mV	26.4 ± 1.0	73.6 ± 2.4	2.2 ± 0.1	0.001
-900 mV	36.1 ± 1.0	63.9 ± 2.4	1.9 ± 0.1	0.001
-1000 mV	70.5 ± 1.0	29.5 ± 2.4	0.9 ± 0.1	0.001
-800 mV_Ox	74.9 ± 0.9	25.1 ± 2.4	0.8 ± 0.1	0.001
-600 mV_Ox	69.8 ± 0.9	30.2 ± 2.4	0.9 ± 0.1	0.001
-400 mV_Ox	55.9 ± 0.9	44.1 ± 2.4	1.3 ± 0.1	0.001
-200 mV_Ox	59.4 ± 0.9	40.6 ± 2.4	1.2 ± 0.1	0.001
0 mV_Ox	49.3 ± 0.9	50.7 ± 2.4	1.5 ± 0.1	0.001

Table S4. Linear combination fit analysis results for in situ XANES spectra of BiSI recorded at the Bi L_{III} edge 1 M KOH solution at various applied potentials.

BiSI	Bi species composition / %		Mean Oxidation state	R_{factor}
	Bi (0)	Bi (III)		
KOH	27.7 ± 5.7	72.3 ± 1.5	2.2 ± 0.1	0.003
-200 mV	23.7 ± 5.7	76.3 ± 1.5	2.3 ± 0.1	0.002
-400 mV	23.7 ± 5.6	77.5 ± 1.3	2.3 ± 0.1	0.002
-600 mV	22.3 ± 5.6	77.7 ± 1.3	2.3 ± 0.1	0.002
-800 mV	41.2 ± 5.7	58.8 ± 1.3	1.8 ± 0.1	0.002
-900 mV	55.0 ± 5.7	45.0 ± 1.3	1.4 ± 0.1	0.003
-1000 mV	77.8 ± 5.6	22.2 ± 1.0	0.7 ± 0.0	0.002
-900 mV_Ox	92.2 ± 5.6	7.8 ± 0.8	0.2 ± 0.0	0.001
-800 mV_Ox	91.3 ± 5.6	8.7 ± 0.8	0.3 ± 0.0	0.001
-700 mV_Ox	90.9 ± 5.5	9.1 ± 0.8	0.3 ± 0.0	0.001
-400 mV_Ox	77.0 ± 5.5	23.0 ± 0.7	0.7 ± 0.0	0.001
-200 mV_Ox	58.7 ± 5.5	41.3 ± 0.6	1.2 ± 0.0	0.001
0 mV_Ox	51.1 ± 0.5	48.9 ± 0.5	1.5 ± 0.0	0.001

Table S5. Linear combination fit analysis results for in situ XANES spectra of the prepared electrodes recorded at the Bi L_{III} edge in absent of electrolyte and any applied potential.

Sample	Bi species composition / %		Mean Oxidation state	R_{factor}
	Bi (0)	Bi (III)		
BiSI-rGO at 0V after 1000cycles	11.0 ± 0.9	89.0 ± 0.9	2.7 ± 0.0	0.001
BiSI at 0V after1000CVscans	38.8 ± 1.0	61.2 ± 1.0	1.8 ± 0.0	0.001

Table S6. Comparison of electrochemical behavior of electrodes.

Sample	Specific capacity ($C\ g^{-1}$)	Electrical conductivity ($S\ cm^{-1}$)	Faradaic efficiency (%)
BiSI-rGO	234	6.32	25.67
BiSI-rGO-1	219	5.48	24.09
BiSI-rGO-2	208	5.97	22.9
BiSI-rGO (1:0.15)	202	6,45	22.15
BiSI-rGO (1:0.1)	232	5.98	24.48
BiSI-rGO (1:0.05)	169	4.12	19.76
BiSI	85	3.73	13.28
BiSI-mix	178	4.81	23.85

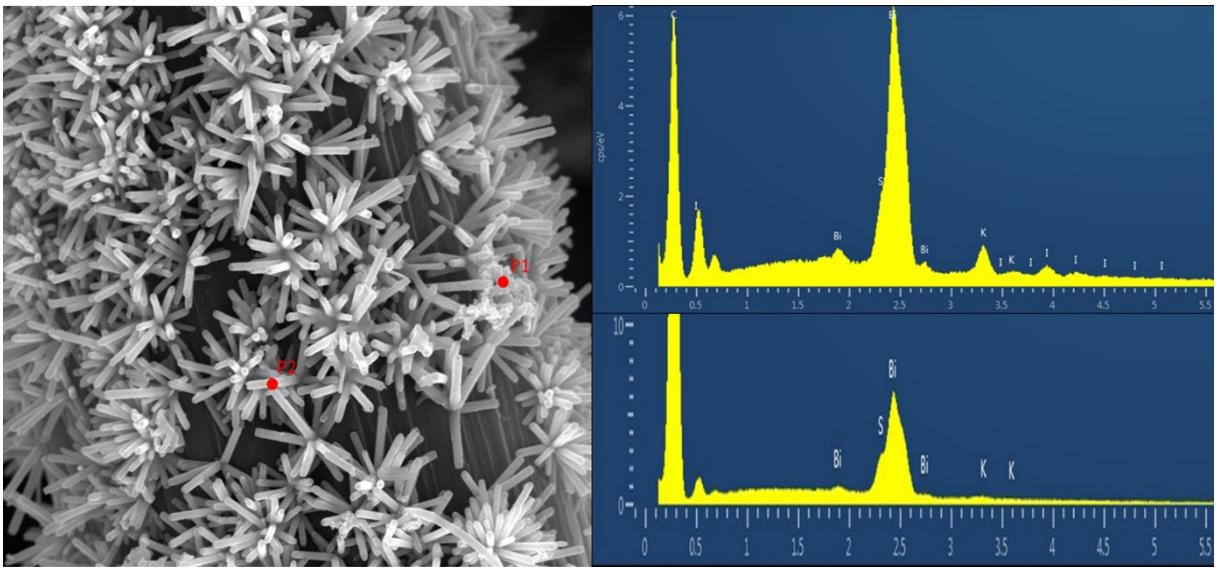

Figure S8. SEM and EDS result of BiSI-rGO electrode after 2000 cycles.

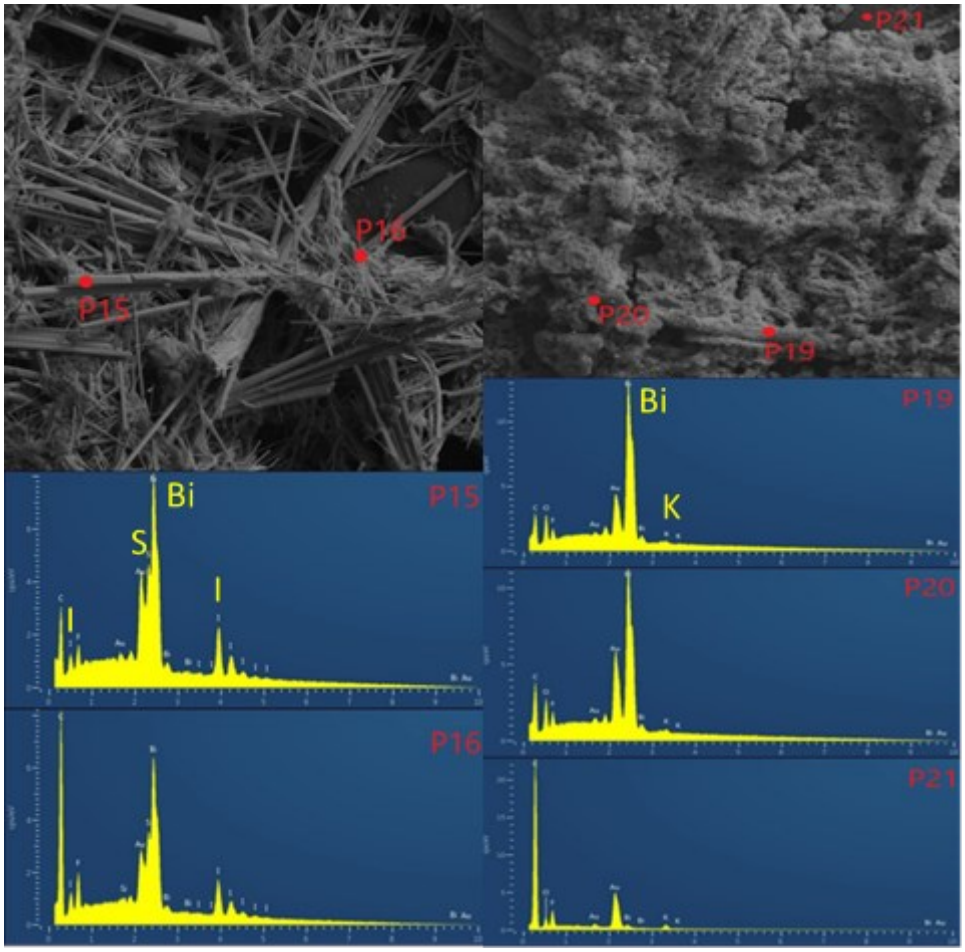

Figure S9. SEM and EDS result of BiSI electrode before cycle, and after 2000 cycles in three electrodes system (from left to right).

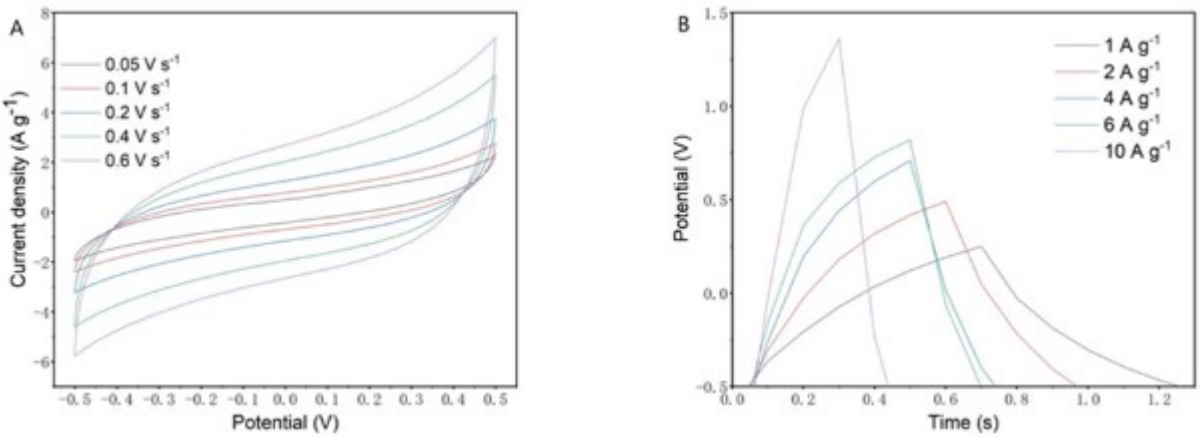

Figure S10 Controlled CV and GCD curve of electrodes.

References

1. S. Brunauer, P. H. Emmett and E. Teller, *Journal of the American chemical society*, 1938, **60**, 309-319.
2. A. M. Wise, P. W. Richardson, S. W. T. Price, G. Chouchelamane, L. Calvillo, P. J. Hendra, M. F. Toney and A. E. Russell, *Electrochimica Acta*, 2018, **262**, 27-38.
3. B. Ravel and M. Newville, *Journal of synchrotron radiation*, 2005, **12**, 537-541.
4. E. Barsoukov and J. R. Macdonald, *Impedance spectroscopy: theory, experiment, and applications*, John Wiley & Sons, 2018.